

Equilibrated polyethylene single-molecule crystals: Molecular-dynamics simulations and analytic model of the global minimum of the free-energy landscape

L Larini^{†‡§¶}, A Barbieri^{†‡}, D Prevosto^{†‡}, P A Rolla^{†‡} and D
Leporini^{†‡§¶}

[†]Dipartimento di Fisica “Enrico Fermi”, Università di Pisa, Largo B.Pontecorvo 3,
I-56127 Pisa, Italy

[‡]INFN, Unità di Ricerca di Pisa, Largo B.Pontecorvo 3, I-56127 Pisa, Italy

[§]INFN-CRS SOFT, Università di Roma La Sapienza, P.zza A. Moro 2, I-00185,
Roma, Italy

[¶] INFN, Unità di Ricerca di Pisa

Abstract. The crystalline state of a single polyethylene chain with $N = 500$ monomers is investigated by extensive MD simulations. The polymer is folded in a well-defined lamella with ten stems of approximately equal length, arranged into a regular, hexagonal pattern. The study of the microscopic organization of the lamella, which is in equilibrium condition, evidenced that the two caps are rather flat, i.e. the loops connecting the stems are short. An analytic model of the global minimum of the free-energy, based on the assumption that the entropic contribution is mainly due to the combinatorics of the stems and loops and neglecting any *conformational* contribution, is presented. It provides for the first time a quantitative explanation of the MD results on the equilibrium geometry of the single-chain crystals.

Submitted to: *J. Phys.: Condens. Matter*

PACS numbers: 61.25.Hq,02.70.Ns

E-mail: dino.leporini@df.unipi.it

¶ To whom correspondence should be addressed.

1. Introduction

The crystalline state of polymers is very different from that of other materials because of the need to arrange in an ordered way a large number of monomers linked to each other sequentially. This results in a wide range of possible hierarchical morphologies where the basic unit is the lamella, which is a few hundred Ångstrom thick [1, 2, 3, 4, 5, 6, 7, 8]. The backbone of a single polymer chain, which is several thousand Ångstrom long, is folded inside the lamella to form the so-called stems; these are perpendicular to the basal surfaces of the lamella where the foldings are localized [4, 5, 6].

Different processes in polymer crystallization are known [1, 2, 4]. Here, we are interested in the *primary homogeneous nucleation* of single-molecule crystals in dilute solutions. The primary nucleation of polymers and oligomers has been investigated in the melt both by experiments [9, 10] and simulations [11]. Nonetheless, very few groups have challenged the rather problematic and related issue of the preparation of single-molecule single crystals [12, 13]. Understanding if the primary nucleation is kinetically or thermodynamically controlled is nontrivial. The difficult characterization of the primary nucleation regime in dilute solutions motivated several simulations [14, 15, 16, 17, 18, 19, 20, 21, 22]. For relatively short chains, the primary nucleation of single-molecule *n*-alkanes with a number of monomers $N = n \leq 300$ were found to end up in the global minimum of the free-energy landscape (FEL), i.e. in thermodynamic equilibrium, at a quench depth $\Delta T \equiv T_m - T \sim 0.2 T_m$, where T_m is the melting temperature [14, 15]. However, the eventual kinetic arrest of the nucleation in one state during the primary nucleation of longer single-molecules cannot be excluded due to the increasing number of entanglements and, consequently, larger energy barriers.

The present paper reports on a simulation, carried out by Molecular-Dynamics (MD) algorithms, of the primary nucleation of single-molecule *n*-alkanes with $N = 500$. Similar lengths are characteristic of polyethylene ($N \gtrsim 200$) more than paraffine waxes ($17 \lesssim N \lesssim 40$) [23]. The goal is to characterize the final crystalline state, which was found to correspond to the global minimum of the FEL [24]. The sharpness of the loops connecting different stems, a feature which is long known [3], is evidenced. Motivated by this finding, a simple analytic model of the FEL global minimum is presented.

2. Numerical methods

The behaviour of a single polyethylene (PE) chain with $N = 500$ monomers in solution has been studied by means of a united-atom model. The chain is described as a sequence of beads, where each bead represents a single methylene CH_2 group. No distinction is made between internal methylene CH_2 groups and terminal methyl CH_3 groups in order to obtain a slight improvement in efficiency [16]. For long chains this approximation is fair. The local interactions shaping the chain are defined by the potentials

$$U_{\text{bond}}(r) = k_r(r - r_0)^2 \quad (1)$$

$$U_{\text{angle}}(\theta) = k_{\theta}(\cos \theta - \cos \theta_0)^2 \quad (2)$$

$$U_{\text{torsion}}(\phi) = k_1(1 - \cos \phi) + k_2(1 - \cos 2\phi) + k_3(1 - \cos 3\phi) \quad (3)$$

$U_{\text{bond}}(r)$ is a harmonic spring potential defined for every couple of adjacent beads, r being their distance and r_0 the equilibrium bond length. $U_{\text{angle}}(\theta)$ is defined for every triplet of adjacent beads, θ being the angle between the corresponding bonds and θ_0 its equilibrium value. Finally, $U_{\text{torsion}}(\phi)$ is defined for every quadruplet of adjacent beads and ϕ is the dihedral angle between the planes defined by the corresponding three adjacent bonds. Pairs of beads not interacting by any of the preceding potentials interact by means of a Lennard-Jones potential

$$U_{\text{LJ}}(r) = 4\epsilon \left[\left(\frac{\sigma}{r} \right)^{12} - \left(\frac{\sigma}{r} \right)^6 \right] \quad (4)$$

with a cutoff radius $r_{\text{cut}} = 2.5\sigma$. The set of parameters of the above force fields are taken from [25] (see table 1). The corresponding time and temperature units are given by $t^* = 2.21$ ps and $T^* = 56.3$ K. All the results will be presented in terms of reduced units. The solvent is mimicked by suitable Langevin dynamics:

$$\ddot{\mathbf{r}}_i = -\nabla_i U - \Gamma \dot{\mathbf{r}}_i - \mathbf{W}_i \quad (5)$$

where \mathbf{r}_i denotes the position vector of the i -th bead, $\nabla_i U$ is the sum of the internal forces acting on it, $\Gamma \dot{\mathbf{r}}_i$ is the frictional force and \mathbf{W}_i is a gaussian noise which sets the temperature via the proper fluctuation-dissipation theorem:

$$\langle \mathbf{W}_i(t) \cdot \mathbf{W}_j(t') \rangle = 6\Gamma k_b T \delta_{ij} \delta(t - t') \quad (6)$$

Equation (5) is integrated by means of the velocity Verlet algorithm with time step $\Delta t = 0.001$ [26]. The runs are performed according to the following protocol: seventeen random chain conformations are initially equilibrated at $T_{\text{eq}} = 15$ for at least ten times the time needed for the self correlation function of the end-to-end vector to vanish. The equilibrated chain does not exhibit any local orientational order. The final temperature $T_f = 9$ is reached via different thermal histories: *i*) instantaneous direct quenches $T_{\text{eq}} \rightarrow T_f$, *ii*) instantaneous quenches with intermediate annealing at T_{ann} , $T_{\text{eq}} \rightarrow T_{\text{ann}} \rightarrow T_f$. Annealing times were 3×10^4 at $T_{\text{ann}} = 9$, 10 and 6×10^4 at $T_{\text{ann}} = 11$. The total number of direct quenches (17) and quenches with intermediate annealing was 28. Having reached T_f , data were collected during evolution times of 3×10^4 . Memory effects were also investigated by preparing a sample in the ‘‘all-trans’’ fully-extended conformation and isothermally annealing it at $T_f = 9$. The all-trans conformation was monitored after the initial preparation for 3×10^4 time units. For all the thermal histories the final crystalline state was found to be independent of the thermal history and, more specifically, to correspond to the global minimum of the FEL [24] in agreement with previous results on shorter chains at the same $T_f = 9$. [14, 15].

3. Results and discussion

Figure 1 shows one conformation of the crystalline state. It is a well-defined lamella with two small-sized caps where the loops connecting the stems are localized. The stems have approximately equal length. Below, it will be seen that they are arranged into a regular, hexagonal pattern and their number μ is well defined ($\mu = 10$). The inertia tensor of the configurations in the final state at $T = 9$ was analyzed. Having ordered the principal axes $\{\mathbf{1}, \mathbf{2}, \mathbf{3}\}$ according to the magnitude of the corresponding eigenvalue, the average values of the three eigenvalues I_1, I_2 and I_3 are $\langle I_1 \rangle = 10097 \pm 58$, $\langle I_2 \rangle = 9885 \pm 51$, $\langle I_3 \rangle = 1148 \pm 11$. Since $\langle I_1 \rangle \gtrsim \langle I_2 \rangle \gg \langle I_3 \rangle$, the ellipsoid of inertia of the crystal exhibits approximate cylindrical symmetry around the $\mathbf{3}$ axis, as it may be also qualitatively seen by visual inspection (see figure 1).

The present model of PE exhibits a local stiffness of the chain over a length scale which is expressed by the Kuhn segment length ℓ_k [1, 2]. The stiffness is apparent in the caps of the crystal where bendings are not smooth but, rather, series of straight sections, see figure 1. One estimates $\ell_k = R_{ee}^2/L \cong 1.2$, corresponding to segments with about four beads, where R_{ee}^2 and L are respectively the mean squared end-to-end distance in the disordered state and the contour length of the polymer. Therefore, the polymer is sketched as a succession of about $N_k = 125$ rigid segments.

3.1. Longitudinal monomer distribution: small caps

In order to analyze the crystal structure one defines the monomer distribution function $\rho(\mathbf{r})$ as

$$\rho(\mathbf{r}) = \frac{1}{N} \sum_{i=1}^N \langle \delta(\mathbf{r} - \mathbf{r}_i^{(\text{cm})}) \rangle \quad (7)$$

where $\mathbf{r}_i^{(\text{cm})}$ is the position of the i -th bead with respect to the center of mass of the chain and the brackets denote a suitable average. In particular, one defines the quantity

$$N_{||}(x^3) = N d \times \int \rho(x^1, x^2, x^3) dx^1 dx^2 \quad (8)$$

where $d \equiv r_0 \sin(\theta_0/2) = 0.31$ is the distance along the chain backbone between two adjacent beads of the fully-extended chain and x^k is the projection of \mathbf{r} along the k -th principal axis. The quantity $N_{||}(z)$ denotes the average number of intersections of the chain with the plane at $x^3 = z$, namely a plane perpendicular to the approximate cylindrical symmetry $\mathbf{3}$ axis. Figure 2 plots the quantity $N_{||}(z)$ for all the thermal histories. It is apparent that the dependence of $N_{||}(z)$ on the thermal history is negligible. In particular, this holds true for the number of stems $\mu = N_{||}(0) = 10$.

Three different regions are seen in figure 2:

- the central region, $|z| \lesssim L_c/2$ with $L_c = 8$, where $N_{||} \simeq 10$;
- the transition region, $L_c/2 \lesssim |z| \lesssim L_c/2 + 2$ where the average orientation of the stems departs from the $\mathbf{3}$ axis;

- the end region, $|z| \gtrsim L_c/2 + 2$, where the stems join each other by forming loops.

Figure 2 shows that the shape of $N_{||}(z)$ is very close to the ideal one corresponding to ten parallel, all-trans stems of fifty monomers each. The comparison makes it more apparent both the order in the final state and the small size of the two crystal caps. In fact, the longitudinal size of the loops, $\Delta z \sim 3$, is fairly smaller than the crystal length $2L_c = 16$. Notice that, since $I_3 \ll I_{\perp}$ with $I_{\perp} = (I_1 + I_2)/2 \simeq 9990$, the folded chain may be sketched as a rigid rod with length $2L$, mass N and negligible thickness. The approximation yields $L = \sqrt{3I_{\perp}/N} \simeq 7.74$, to be compared with $L_c \sim 8$, as drawn from figure 2.

3.2. Transverse monomer distribution: surface mobility

In order to study the monomer distribution in planes perpendicular to the **3** axis one defines

$$\rho_{\perp,\text{centr}}(\mathbf{x}_{\perp}) = \int_{-L_c/2}^{L_c/2} \rho(\mathbf{x}_{\perp}, z) dz \quad (9)$$

$$\rho_{\perp,\text{trans}}(\mathbf{x}_{\perp}) = \int_{L_c/2}^{L_c/2+2} [\rho(\mathbf{x}_{\perp}, z) + \rho(\mathbf{x}_{\perp}, -z)] dz \quad (10)$$

$$\rho_{\perp,\text{term}}(\mathbf{x}_{\perp}) = \int_{L_c/2+2}^{\infty} [\rho(\mathbf{x}_{\perp}, z) + \rho(\mathbf{x}_{\perp}, -z)] dz \quad (11)$$

where $\mathbf{x}_{\perp} = x^1 \mathbf{1} + x^2 \mathbf{2}$ denotes the position vector in the transverse plane. $\rho_{\perp,\text{centr}}(\mathbf{x}_{\perp})$, $\rho_{\perp,\text{trans}}(\mathbf{x}_{\perp})$ and $\rho_{\perp,\text{term}}(\mathbf{x}_{\perp})$ are the transverse monomer distributions in the central, transition and end regions, respectively. Figure 3 shows the topography of the crystal structure. The ten stems of the crystalline nucleus arrange themselves into an hexagonal structure (top plot). Noticeably, there is virtually no order on the crystal surface. Moving to the caps of the crystal structure the amount of order decreases. The transition region (center plot) still retains a partially ordered structure, visible in the two central stems, whereas the remaining eight external stems become more mobile. In the end regions (bottom plot), where the loops connecting the stems are located, any ordered structure is lost. The presence of a disordered ‘‘corona’’ surrounding the ordered fraction of the nucleus has been noted by MonteCarlo simulations [17]. In the present case the direct inspection of several snapshots shows that the crystal surface is highly mobile and includes the chain ends, the so called cilia, which are excluded from the crystal interior. The confinement of the cilia on the surface avoids the impairment of lattice perfection and agrees with previous experimental findings [3].

4. Analytic model of the FEL global minimum

The experimental evidence suggests that long alkanes fold in integral reciprocals of the extended chain length. In particular, this implies that large portions of the chain are mostly contributing to the straight stems, i.e. the size of the loops connecting different

stems is short [3]. In our simulations, this is apparent from selected configurations, (figure 1) as well as from the analysis of the longitudinal monomer distribution (figure 2). The average length of the loops ℓ_{loop} is relatively small and involves a short sequence of Kuhn segments, $\ell_{\text{loop}}/\ell_k \sim 4$ [24]. Based on these remarks, a very simple model which incorporates the above feature and accounts for the existence of equilibrium folded structures has been developed.

A crystallized chain of N_k Kuhn segments is pictured as formed by a nucleus with μ stems, $\mu - 1$ loops and the two cilia. When a segment is included in one stem of the nucleus the energy gain is $\varepsilon > 0$ in units of kT . The lateral surface free-energy contribution per unit area is σ' in units of kT . If m denotes the average number of segments per stem, the overall free-energy $F_{m,\mu}$ of the nucleus is written as:

$$\frac{F_{m,\mu}}{kT} = -\mu m \varepsilon + \sigma \sqrt{\mu} m - \ln W_{m,\mu} \quad (12)$$

with $\sigma = \alpha \sigma' r_0^2$, α being a numerical factor. $W_{m,\mu}$ denotes the number of distinct ways to arrange the N_k segments in μ stems, each of m segments, $\mu - 1$ loops and two tails. To evaluate $W_{m,\mu}$ one assumes that each loop has only one conformation. This roughly accounts for the both the expected stiffness of the short loops and their mutual steric constraints. We factorize $W_{m,\mu}$ as

$$W_{m,\mu} = \binom{N_k - \mu m + \mu}{\mu} \times p^{\mu-1} \quad (13)$$

The binomial coefficient enumerates the distinct ways to get a one-dimensional arrangement of $(N_k - \mu m)$ segments separated by μ walls. The second term is a weighting factor accounting for the entropic limitations to bend the linear arrangement and form a crystalline nucleus with $\mu - 1$ loops. One expects that conformations with a large number of loops are inhibited by jams occurring in the compact caps of the nucleus (see figure 1). Owing to the roughness of the present model p is left as an adjustable parameter.

Equation (13) sets the entropic contribution $\ln W_{m,\mu}$ to the free energy. Small variants, e.g. by neglecting the two cilia, do not improve the model appreciably. Muthukumar proved that the entropy role is crucial to enforce the minimum of $F_{m,\mu}$ and estimated $W_{m,\mu}$ by resorting to a gaussian model of the loops and to a field-theoretic approach [15]. Although the gaussian model is expected to work nicely for long loops, it may overestimate $W_{m,\mu}$ in the case of short loops. The present model cuts the entropy due to the loop conformations, i.e. the so called entropy of disorientation, and limits the entropy to the mixing of the μ stems of the crystalline nucleus (with m segments each) along the polymer chain. The resulting free-energy has one adjustable parameter less than the one of reference [15].

Representative plots of the free-energy-landscape (FEL) and the contour plot of the minimum are shown in figures 4 and 5, respectively. Qualitatively similar plots were also presented in [15]. The FEL is limited to the region $\mu m < N_k$ where segments are

available to form both the loops and the two cilia. At $\mu m \lesssim N_k$ a steep ridge is found, due to the small entropy of conformations with very short loops/cilia. Figure 5 shows the contour plots of the FEL of figure 4. The minimum is located at $m^* = 9.68, \mu^* = 9.94$. This must be compared with $\mu = 10$ from the MD results. If L_{stem} is the stem length, the average number of Kuhn segments per stem is $m = L_{\text{stem}}/\ell_k$. From figure 2 one estimates $L_{\text{stem}} = 2z^*$, where z^* is the positive non trivial solution of the equation $N_{||}(z) = 10$, i.e. the intercept with $z \neq 0$ between the distributions $N_{||}(z)$ from the simulation and the one from the ideal case of ten fully stretched stems. One finds $m = 10$ with $L_{\text{stem}} = 12$, to be compared with $m^* = 9.68$ of the model. Finally, one notes that the coordinates of the FEL minimum correspond to an average number of segments located in each loop equal to $(N_k - \mu^* m^*)/(\mu^* - 1) = 3.22$. The value is consistent with the basic assumption of the model, i.e short loops, and compares well with the value from the MD simulations, about 3 – 4 [24].

Figure 6 is a parametric plot of the number of stems $\mu^*(\varepsilon, \sigma)$ and the segments per stem, $m^*(\varepsilon, \sigma)$ of the FEL minimum with $p = 0.06$ for different ε and σ values. On increasing the surface tension σ , the minimum moves from very prolate crystals (few and very long stems) to more spherical crystals (more and shorter stems) to minimize the exposed surface by keeping the total volume constant (N_k constant). The presence of a maximum number of stems for a given ε must be considered with caution, in that it corresponds to a very small number of segments per stem and a to very large number of segments located in the loops, therefore pushing the model to its limits.

The existence of a minimum of $F_{m,\mu}$ relies on the limitations to have conformations with large number of loops. This is understood by noting the relation $F_{m,\mu} = F_{m,\mu}(p=0) - (\mu - 1) \ln p$ ($p < 1$) which makes explicit the entropic penalty for conformations with large number of stems μ . In fact, if the entropy penalty is removed by setting $p = 1$, $F_{m,\mu}$ with the same parameters of figure 4 has no minimum (data not shown). At constant p , the minimum disappears at high temperatures (small ε and σ). As an example, for $N_k = 125$, $p = 0.06$ and $\sigma/\varepsilon = 0.22, 2.2, 3$ the minimum disappears for $\varepsilon < 0.062, 0.2953, 0.8275$, respectively. This shows that increasing σ enforces higher energy gain ε to make the crystal nucleus stable. Note the approximate scaling σ/ε^2 .

5. Conclusion

The paper has presented numerical results from extensive MD simulations of the crystallization process of a single PE chain with $N = 500$ monomers. The chain, after suitable equilibration at high temperature is cooled at the final temperature $T_f = 9$ by quenches involving or not intermediate annealing steps. The chain is also isothermally annealed at T_f after initial preparation in the fully-stretched “all-trans” configuration. No dependence on the thermal history was observed at late stages of the crystallization process which eventually yields a well-defined equilibrated lamella with ten stems of approximately equal length, arranged into a regular, hexagonal pattern. The study of the microscopic organization of the lamella evidenced that the two caps are rather

flat, i.e. the loops connecting the stems are short. It is also seen that the chain ends, the so-called cilia, are localized on the surface of the lamella, in agreement with the experiments [3], and that structural fluctuations take place on the lamella surface, as noted by recent MonteCarlo simulations [17]. Motivated by the MD finding that the lamella is in the equilibrium state and that the caps of the lamella are rather small, an analytic model of the global minimum of the FEL, based on the assumption that the entropic contribution is mainly due to the combinatorics of the stems and of the loops, i.e. neglecting any *conformational* contribution, is developed. It provides for the first time a quantitative explanation of the MD results on the equilibrium geometry of the single-chain crystals.

Acknowledgments

Financial support from MIUR within the PRIN project “Dynamics and Thermodynamics in out-of-equilibrium materials: structural glasses, gels, polymeric materials” is gratefully acknowledged.

References

- [1] Gedde U W 1995 *Polymer Physics* (London: Chapman and Hall)
- [2] Strobl G 1997 *The Physics of Polymers* (New York: Springer Verlag)
- [3] Ungar G, Stejny J, Keller A, Bidd I and Whiting M C 1985 *Science* **229** 386
- [4] Armitstead K and Goldbeck-Wood G 1992 *Adv. Polym. Sci.* **100** 219
- [5] Keller A 1968 *Rep. Prog. Phys.* **31** 623
- [6] Philips P J 1990 *Rep. Prog. Phys.* **53** 549
- [7] Strobl G 2000 *Eur. Phys. J. E* **3** 165
- [8] Muthukumar M 2000 *Eur. Phys. J. E* **3** 195
- [9] Organ S J, Keller A, Hikosaka M and Ungar G 1996 *Polymer* **37** 2517
- [10] Ghosh S K, Hikosaka M, Toda A, Yamazaki S and Yamada K 2002 *Macromolecules* **35** 6985
- [11] Gee R H and Fried L E 2003 *J. Chem. Phys.* **118** 3827
- [12] Bu H, Pang Y, Song D, Yu T, Voll T M, Czornyj G and Wunderlich B 1991 *J. Polymer Sci., Part B: Polym. Phys.* **29** 139
- [13] Liu L Z, Su F Y, Zhu H S, Li H, Zhou E L, Yan R F and Qian R Y 1997 *J. Macromol. Sci., Phys. B* **36** 195
- [14] Welch P and Muthukumar M 2001 *Phys. Rev. Lett.* **87** 218302
- [15] Muthukumar M 2003 *Phil. Trans. R.Soc. Lond. A* **361** 539
- [16] Liu C and Muthukumar M 1998 *J. Chem. Phys.* **109** 2536
- [17] Hu W, Frenkel D and Mathot V B F 2003 *J. Chem. Phys.* **118** 3455
- [18] Hu W, Frenkel D and Mathot V B F 2003 *Macromolecules* **36** 8178
- [19] Kavassalis T A and Sundararajan P R 1993 *Macromolecules* **26** 4144
- [20] Sundararajan P R and Kavassalis T A 1995 *J. Chem. Soc. Faraday Trans.* **91** 2541
- [21] Fujiwara S and Sato T 2001 *J. Chem. Phys.* **114** 6455
- [22] Fujiwara S and Sato T 1999 *J. Chem. Phys.* **110** 9757
- [23] Kraack H, Deutsch M and Sirota E B 2000 *Macromolecules* **33** 6174
- [24] Larini L, Barbieri A and Leporini D 2005 *to be submitted*
- [25] Muthukumar M and Welch P 2000 *Polymer* **41** 8833
- [26] Allen M P and Tildesley D J 1987 *Computer Simulation of Liquids* (Oxford: Clarendon Press)

Tables

Parameter	Value	
	reduced units	SI units
ϵ	1	0.112 kcal/mol
σ	1	4.04 Å
m	1	14.03 g/mol
Γ	1	0.455 s^{-1} /mol
k_r	51005	350 kcal/mol Å ²
r_0	0.38	1.53 Å
k_θ	535.71	60 kcal/mol
θ_0	109°	109°
k_1	26.96	3.02 kcal/mol
k_2	-5	-0.56 kcal/mol
k_3	23.04	2.58 kcal/mol

Table 1. Parameters of the force field.

Figure captions

Figure 1. Wire-frame view of one conformation of the single-molecule crystal. Note the short loops connecting the stems.

Figure 2. The number of intersections of the chain in the crystalline state with the plane at $\mathbf{3} = z$, $N_{||}(z)$. The plane is perpendicular to the approximate cylindrical symmetry axis x^3 . The curves refer to the different thermal histories. The dashed line is the distribution corresponding to the ideal case of ten parallel and fully extended stems with fifty monomers each. The number of stems μ is equal to $N_{||}(0) = 10$. Note the steep decrease at the end regions evidencing the small size of the loops connecting the stems.

Figure 3. Topographic view of the crystal state via the transverse distributions $\rho_{\perp,\text{centr}}$ (top), $\rho_{\perp,\text{trans}}$ (center) and $\rho_{\perp,\text{term}}$ (bottom) (equations (9-11)). Note the absence of ordered structures on the crystal surface and the two caps.

Figure 4. The free-energy landscape (FEL) of the model. m is the number of Kuhn segments belonging to one of the μ stems. $N_k = 125$, $\varepsilon = 0.6$, $\sigma = 0.97$, $p = 0.06$.

Figure 5. Contour plot of the FEL of figure 4. The minimum is located at $m^* = 9.68$, $\mu^* = 9.94$.

Figure 6. Plot of the coordinates μ^* , m^* of the FEL minimum with $N_k = 125$, $p = 0.06$ for different ε and σ values. For $\varepsilon = 0.4, 0.6, 0.8$, σ is in the intervals $0.5 \leq \sigma \leq 0.95$, $0.6 \leq \sigma \leq 1.655$, $0.8 \leq \sigma \leq 2.4$, respectively. m^* always decreases by increasing σ .



FIGURE 1

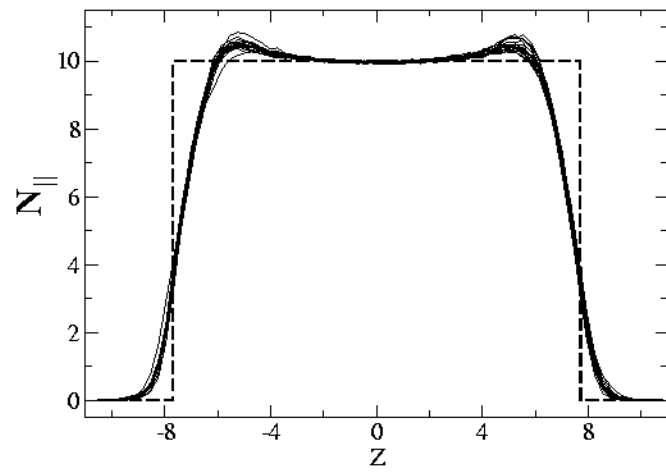


FIGURE 2

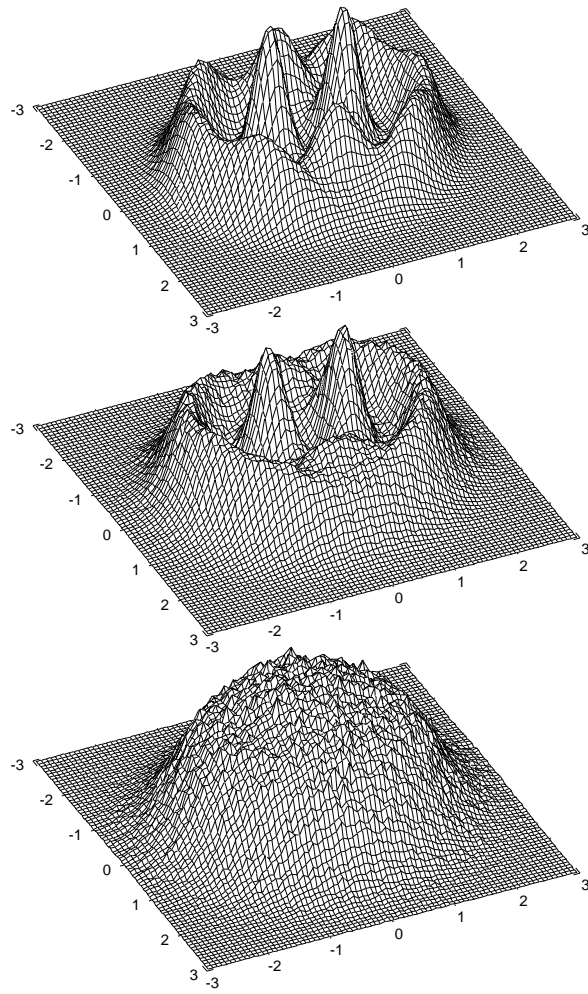


FIGURE 3

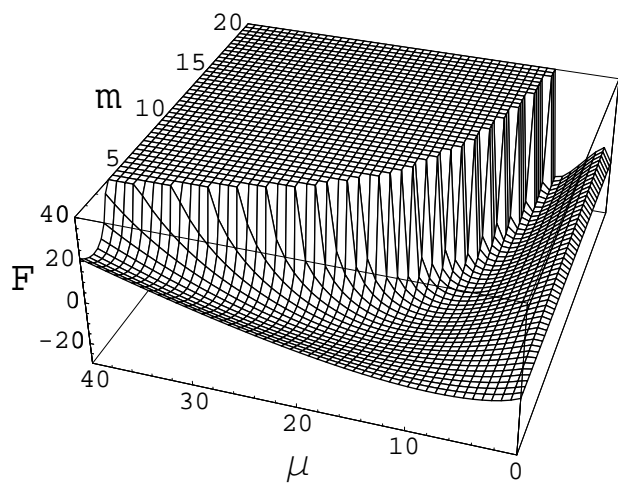


FIGURE 4

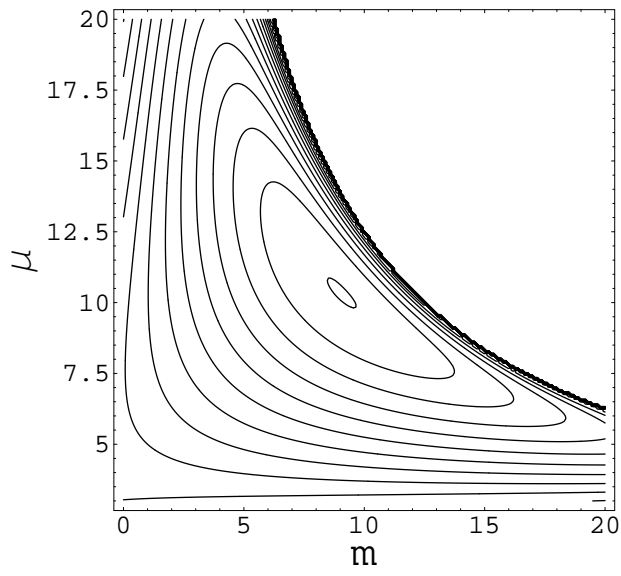


FIGURE 5

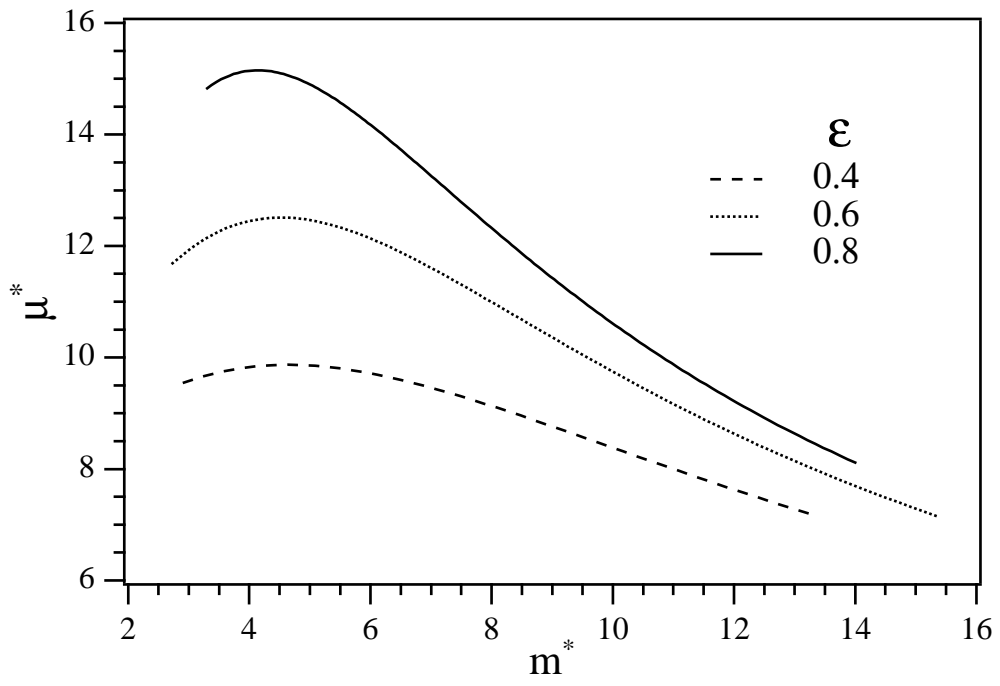


FIGURE 6